

REDUCTION OF DETAILED CHEMICAL REACTION NETWORKS FOR DETONATION SIMULATIONS

Patrick Hung
Mechanical Engineering
California Institute of Technology
Pasadena, CA 91125

Joseph E. Shepherd
Graduate Aeronautical Laboratory
California Institute of Technology
Pasadena, CA 91125

While a detailed mechanism represents the state-of-the-art of what is known about a reaction network, its direct implementation in a fully resolved CFD simulation is all but impossible (except for the simplest systems) with the computational power available today. This paper discusses the concept of Intrinsic Low Dimensional Manifold (ILDm), a technique that systematically reduces the complexity of detailed mechanisms. The method, originally developed for combustion systems, has been successfully extended and applied to gaseous detonation simulations^{2,3,4}. Unfortunately, while a one-dimensional ILDM is reasonably easy to compute, manifolds of higher dimensions are notoriously difficult. Moreover, the selection of the manifold dimension has been largely arbitrary, with a one-dimensional ILDM being the most popular if for no other reason than that it is easiest to compute and store.

In this paper, we will present a technique that enables us to quantitatively determine the dimensionality of the ILDM needed, as well as a robust and embarrassingly parallel algorithm for computing high-dimensional ILDMs. Finally, these techniques are demonstrated in the context of a one-dimensional ZND detonation with detailed chemistry.

INTRODUCTION

Intrinsic Low Dimensional Manifold (ILDM) is a technique for systematically identifying low-dimensional attracting submanifolds of the original state space of chemical reaction mechanisms¹. The method, originally developed for low-speed combustion systems, has been successfully extended and applied to two-dimensional gaseous detonation simulations with the Hydrogen-Oxygen reaction mechanism², and gaseous detonation³ and gas phase RDX combustion⁴. While detailed reaction mechanisms are now mature for many hydrocarbon fuels and in a developmental stage for nitramine explosives such as RDX and HMX, a number of issues remain to be addressed before they can be used in conjunction with the ILDM method for detonation simulation.

First, the ILDM algorithm is computationally expensive to apply, and the computed manifold presents difficult tabulation, storage, and interpolation problems. While a one-dimensional ILDM can be computed reasonably easily and has been shown to work well for simple reaction systems such as the Hydrogen-Oxygen reaction mechanism, it is not reasonable to expect such drastic amount of reduction to remain faithful to even moderately complex hydrocarbon mechanisms. We will present an algorithm that allows us to determine, quantitatively, the number of dimensions needed. The reason for using ILDMs in detonation simulation is simple; we want to extract as much information from the detailed mechanism as we can afford, and as little as we need. The ILDM technique allows us to follow (if not reach) this goal systematically. Unfortunately, algorithms for computing ILDMs, the most popular being continuation methods, are far from robust. In this paper, a new algorithm for the computation of ILDMs that is more efficient, embarrassingly parallel, and far more robust than continuation methods is presented.

Finally, these techniques are applied to a one-dimensional ZND detonation, giving us valuable insights as well as demonstrating clearly a “stepping-down” of dimensions as we move away from the leading shock front. In other words, the closer to the front we need to capture the reaction dynamics, the higher the dimension we need. Finally, remarks concerning the application of this technique, as well as ramifications of some of the underlying assumptions, are discussed.

INTRINSIC LOW DIMENSIONAL MANIFOLDS

By using an operator split scheme to the reactive Euler equations², each of the finite volume in the discretized domain during the reaction source step is a constant-volume adiabatic combustor. The governing equation is a system of ODE, which can be written as,

$$\frac{d\bar{\phi}}{dt} = \bar{f}(\bar{\phi}; \rho, e) \quad (1)$$

where

$$\bar{\phi} = (\phi_1, \phi_2, \dots, \phi_n)^T, \quad \phi_k = \frac{y_k}{W_k}$$
$$\bar{f} = \left(\frac{\omega_1}{\rho}, \frac{\omega_2}{\rho}, \dots, \frac{\omega_n}{\rho} \right)$$

ϕ_k is the specific mole number of species k (with units [mol/kg]). The density ρ and specific internal energy e appear as parameters to the governing ODE. The total number of species in the reaction mechanism is denoted by n , which is also the dimensionality of the chemical state-space.

The definition of the ILDM is given below. Given a vector field \bar{f} , the Jacobian matrix is defined below.

$$J(\bar{\phi}) = \frac{\partial \bar{f}}{\partial \bar{\phi}}, \quad J_{i,j} = \bar{f}_{i,j} \quad (2)$$

The Jacobian can then be transformed into a basis consisting of a direct sum of two subspaces⁵,

$$J(\bar{\phi}) = (Z_s Z_f) \begin{pmatrix} \Lambda_s & 0 \\ 0 & \Lambda_f \end{pmatrix} \begin{pmatrix} \hat{Z}_s \\ \hat{Z}_f \end{pmatrix}$$

with,

$$\begin{pmatrix} \hat{Z}_s \\ \hat{Z}_f \end{pmatrix} = (Z_s \quad Z_f)^{-1}$$

where Z_s is a column partitioning of vectors spanning the slow subspace, defined to be the invariant eigenspace of J associated with the least negative eigenvalues. A different basis, in particular an orthonormal one, can be used instead. Z_f is defined analogously, being spanned by the remaining eigenvectors of J .

The equation that defines the ILDM is, finally,

$$\hat{Z}_f \bar{f}(\bar{\phi}) = \bar{0} \quad (3)$$

Or more formally, to seek a k -dimensional ILDM, denoted by \mathfrak{M}^k , we have:

$$\mathfrak{M}^k = \{ \bar{\phi} : \hat{Z}_f \bar{f}(\bar{\phi}) = \bar{0} \} \quad (4)$$

where

$$\hat{Z}_f \bar{f} : \mathbb{R}^n \rightarrow \mathbb{R}^{n-k} \quad (5)$$

This definition is numerically awkward for the following reasons. The ILDM is defined as the zero level-set of a complicated nonlinear system. One-dimensional level-sets are not difficult to find by continuation methods, but higher dimensional level-surfaces are tricky, to put it mildly.

Next, we have an additional complication from mass conservation. Each (independent) elemental constraint increases the multiplicity of the zero eigenvalue by one. Given m (independent) elemental constraint and assume we are seeking a k -dimensional ILDM, a remedy is to solve for

$$\mathfrak{M}^{k+l} \cap N_{ij} \phi_j = N_{ij} \phi_i^o \quad (6)$$

where N_{ij} is the (m by n) species-element matrix, and ϕ_i^o denotes some initial composition. This is discussed in some detail by Eckett².

Finally, and perhaps most importantly, the defining function $\hat{Z}_f \bar{f}$ is highly nonlinear. Being a composite function where \hat{Z}_f comes possibly from matrix inversion, the null space of $\hat{Z}_f \bar{f}$, needed for continuation procedures, is difficult to find accurately and needs to be approximated.

THE ILDM RECASTED

The disadvantages above notwithstanding, the ILDM as formulated originally does have an advantage: it suggests a direct method of solving for \mathfrak{M}^k , as long as we can compute level-surfaces.

By examining Eq. (4), we see that a point $\bar{\phi}$ in chemical state space is in \mathfrak{M}^k when $f(\bar{\phi})$, transformed to the new basis $(Z_s Z_f)$, has no components in the fast subspace. In other words, we have

$$\bar{\phi} \in \mathfrak{M}^k \Leftrightarrow \bar{\phi} \in \text{span}\{Z_s\} \quad (7)$$

Eq. (7) has a very desirable property: only right eigenvectors are needed to compute a basis for Z_s . Although not a *constructive* definition of \mathfrak{M}^k , Eq. (7) poses, as well as provides an answer to, the important inverse question: What is the ILDM-dimensionality of $\bar{\phi}$? We will define the ILDM-dimension of $\bar{\phi}$, denoted by $\text{ILDM-dim}(\bar{\phi})$, by

$$\text{ILDM-dim}(\bar{\phi}) = \min(k) : \bar{\phi} \in \mathfrak{M}^k \quad (8)$$

The ILDM-dimension is well-defined because of the (trivial) inclusion property:

$$\mathfrak{M}^0 \subseteq \mathfrak{M}^1 \subseteq \dots \subseteq \mathfrak{M}^n \quad (9)$$

We will see how this ILDM-dimension can be computed in the next section.

ILDM-DIMENSIONALITY AND THE GRAMMIAN PROCEDURE

We can use the original definition of the ILDM to compute $\text{ILDM-dim}(\bar{\phi})$ by writing $f(\bar{\phi})$ in a sorted eigenbasis and counting the number of zeros, but this is numerically ill-posed, in part because of numerical imprecision and round-off errors, and more importantly, because \mathfrak{M}^k is not an invariant manifold (see the concluding remarks for more details).

Eq. (8) does provide us with a viable, and direct, algorithm for estimating $\text{ILDM-dim}(\bar{\phi})$. We define the k -dimensional Gram determinant (or Grammian⁶) of $\bar{\phi}$, denoted by $\Gamma^k(\bar{\phi})$, by

$$\Gamma^k(\bar{\phi}) = \det(A^T A) \quad (10)$$

where A is an $n \times (k+1)$ matrix consisting of a column partitioning of the k slowest eigenvector, augmented by an arc-length normalized $f(\bar{\phi})$,

$$A = (v_1, v_2, \dots, v_n, g(\bar{\phi})) \quad (11)$$

where

$$g(\bar{\phi}) = f(\bar{\phi}) / \|f(\bar{\phi})\| \quad (12)$$

This definition of $\Gamma^k(\bar{\phi})$ satisfies the inclusion relation of Eq. (9):

$$\Gamma^i(\bar{\phi}) \leq \Gamma^j(\bar{\phi}), \quad \forall i > j \quad (13)$$

Additionally, the Gram determinant is non-negative and bounded above by one,

$$1 \geq \Gamma^i(\bar{\phi}) \geq 0, \quad \forall i \quad (14)$$

Furthermore, $\Gamma^k(\bar{\phi})$, viewed as a scalar valued function on $(k+1)$ vectors, is continuous.

Finally, we have a method of computing $\text{ILDM-dim}(\bar{\phi})$, as follows

$$\text{ILDM-dim}(\bar{\phi}) = \min(k) : \Gamma^k < \varepsilon \quad (15)$$

Note that the $\text{ILDM-dim}(\bar{\phi})$ in Eq. (15) depends on a parameter ε , exactly analogous to the concept of the numerical rank⁷ (ε -rank) for matrices.

We will illustrate this technique by computing the ILDM-dimension along a constant-volume reaction trajectory. Given an ODE of the form Eq. (1), subject to some initial conditions $\bar{\phi}^o$, the reaction trajectory $\bar{\phi}(t)$ satisfies,

$$\begin{aligned} \bar{\phi}(0) &= \bar{\phi}^o \\ \frac{d}{dt} \bar{\phi}(t) &= f(\bar{\phi}(t); \rho, e) \end{aligned} \quad (16)$$

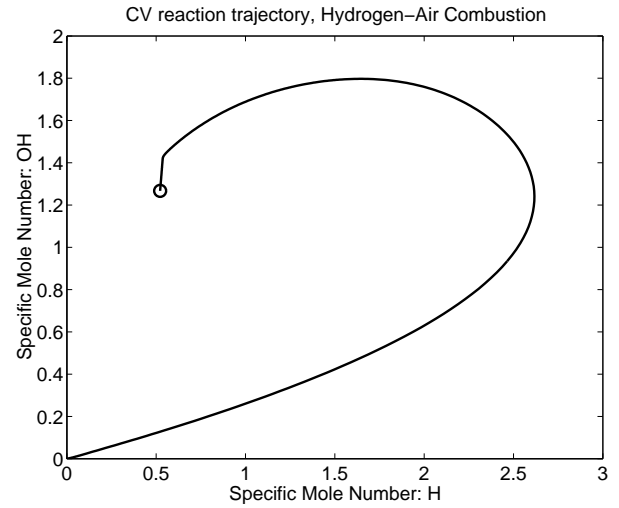


Figure 1. Constant-volume trajectory for Hydrogen-Air Combustion.

Figure 1 shows a constant-volume trajectory for the stoichiometric combustion of Hydrogen-Air ($2\text{H}_2 + \text{O}_2 + 3.76\text{N}_2$) with a density of 4.58 kg/m^3 and a specific internal energy 1.27 MJ/kg . These conditions correspond to an initial temperature of 1543.4 K and an initial pressure of 2.8104 MPa . These conditions are taken from Eckett² and correspond approximately to the von Neumann state of a CJ detonation of the mixture.

The first three Gram determinants along the trajectory, i.e. $\Gamma^m(\bar{\phi}(t))$, $m=1,2,3$ are shown in Figure 2. This figure has two interesting interpretations.

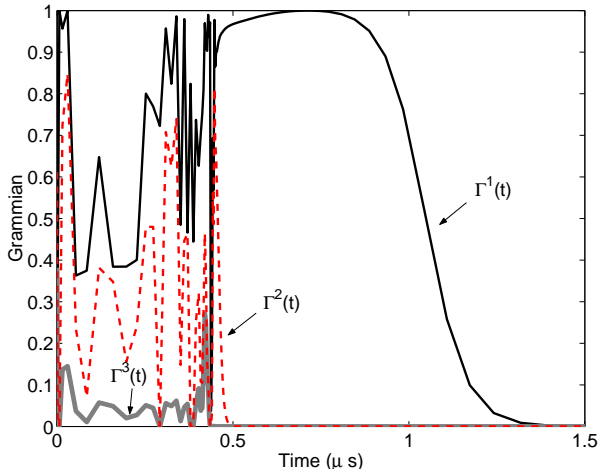


Figure 2: The first three Gram Determinants along the CV trajectory of Figure 1 are plotted as a function of time.

It can be seen, for example at 1 microsecond, the only non-zero Gram determinant is Γ^1 . This follows from Eq. (15) that the ILDM-dimensionality of the trajectory at that instant is 2. It means that when $\Gamma^2 \leq \varepsilon$ and $\Gamma^1 > \varepsilon$, the two slowest eigenvectors are necessary and sufficient to span $f(\bar{\phi})$.

The alternate point of view is the concept of the time of arrival, introduced below. We will define the *time of arrival* t_k of a trajectory $\bar{\phi}(t)$ to \mathfrak{M}^k by

$$\min(t_k) : \Gamma^k(\bar{\phi}(t)) \leq \varepsilon \quad \forall t > t_k \quad (17)$$

It can be seen from Figure 2, with the definition provided by Eq. (17), that the time of arrival to $\mathfrak{M}^3, \mathfrak{M}^2, \mathfrak{M}^1$ is, approximately, 0.4, 0.5 and 1.5 microseconds, respectively.

Figure 3 decorates the reaction trajectory from Figure 1 with the ILDM-dimension estimated by the Grammian procedure. As will be seen shortly, this ability to compute the ILDM-dimension of any point $\bar{\phi}$ in chemical state-space forms the basis of our proposed embarrassingly parallel algorithm for ILDM computations.

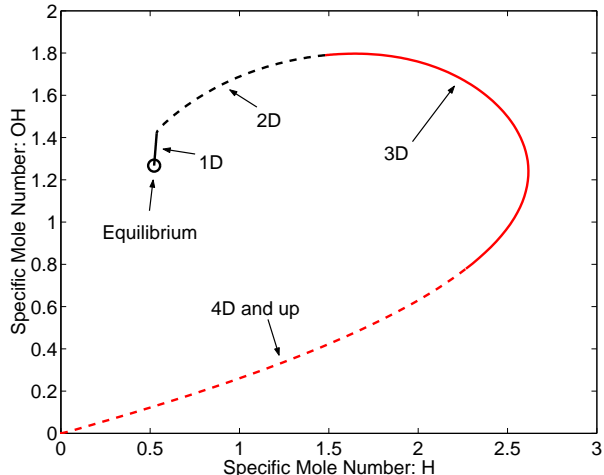


Figure 3: The ILDM dimension is shown along the CV trajectory of Figure 1.

ILDM VIA CONGRUENCES

The definition of ILDM through Eq. (4) provides, by rewriting it in explicit form, a direct method of computing \mathfrak{M}^k ,

$$\mathfrak{M}^k = (\hat{Z}_f \bar{f})^{-1}(\bar{0}) \quad (18)$$

It is important to note what is meant by a (numerical) solution of Eq. (18). Generally, a solution is comprised of a set of points S , perhaps tabulated with some predetermined parameterizations, in the original n -dimensional chemical state space, with each point satisfying Eq. (3) to within some tolerance:

$$\|\hat{Z}_f \bar{f}(\bar{\phi})\| \leq \varepsilon, \quad \forall \bar{\phi} \in S \quad (19)$$

Numerical schemes based on continuation methods are typically used to solve Eq. (18), which becomes very difficult for $k > 1$.

On the other hand, armed with the tools from the previous sections for computing the ILDM-dimension, it is possible to take an indirect approach. We will redefine the set S as:

$$\Gamma^k(\bar{\phi}) \leq \varepsilon, \quad \forall \bar{\phi} \in S \quad (20)$$

Given a trajectory $\bar{\phi}(t)$ satisfying Eq. (1) subject to some initial condition $\bar{\phi}^o$, we compute the time of arrival of $\bar{\phi}(t)$ to t_k to \mathfrak{M}^k , as de-

fined in Eq. (17). Together with Eq. (20), we see that

$$\bar{\phi}(t) \in S, \forall t \geq t^k \quad (21)$$

In other words, we can solve \mathfrak{M}^k (populate the set S) by solving Eq. (1) subjected to different initial conditions. This “filling of a manifold” by curves is called a congruence⁸.

EXAMPLE: CONSTRUCTION OF A ONE-DIMENSIONAL ILDM

We will use our procedure described above to compute the one-dimensional ILDM for the detonation problem studied in Rastigejev et al⁹. We will represent the system by Eq. (1), repeated below,

$$\frac{d\bar{\phi}}{dt} = \bar{f}(\bar{\phi}; \rho, e) \quad (22)$$

We will proceed as follows. A one-dimensional ILDM \mathfrak{M}^1 is, roughly speaking, a line through the equilibrium point in chemical state-space. Using any point $\bar{\phi}^o \in \mathfrak{M}^1$ as initial data to Eq. (22), the trajectory that results will be a part of \mathfrak{M}^1 , starting at $\bar{\phi}^o$ and ending at equilibrium.

The equilibrium point therefore divides \mathfrak{M}^1 into two pieces. Our procedure that follows will determine, in the linear approximation, the two initial data (one on each side of the equilibrium) that maximize the extent of our solution to \mathfrak{M}^1 .

We first compute the one-dimensional slow eigenspace of the system, which is an affine linear space centered at the equilibrium point spanned by the slowest eigenvector. This is shown in Figure 4.

The meaning of this eigenspace, which we will denote by L^1 for convenience, is well known and will not be elaborated. In the neighborhood of the equilibrium point, \mathfrak{M}^1 is tangent to L^1 .

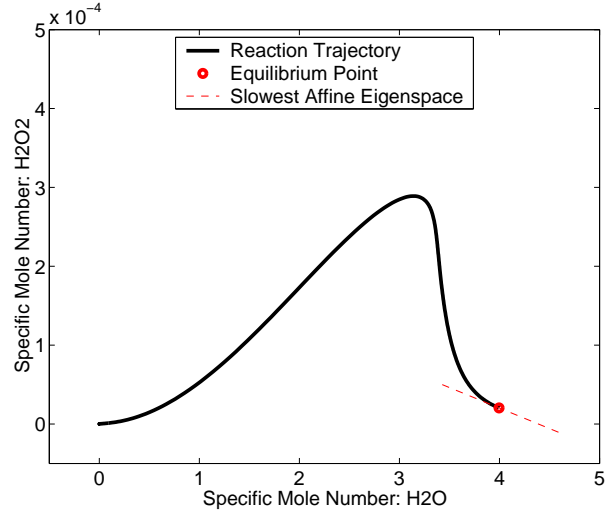


Figure 4 CV Reaction trajectory, equilibrium point and the slowest linear eigenspace.

Chemical state-space is compact as it is subjected to the positivity constraint

$$\phi_i \geq 0, \forall i = 1..n \quad (23)$$

as well as elemental conservation

$$N_{ij}\phi_j = N_{ij}\phi_j^o \quad (24)$$

where, as alluded to earlier, N_{ij} is the species-element matrix. Eq. (24) is automatically enforced in the solution of Eq. (22) because, when each of the reactions in the detailed mechanism conserves elements,

$$\bar{f}(\bar{\phi}) \in \text{Null}(N_{ij}) \quad (25)$$

The maximum extent of L^1 is a problem in linear programming. In one-dimension, it is akin to extending L^1 until one of the n inequalities in Eq. (23) becomes an equality. The range of validity for the thermodynamic data imposes an additional constraint: at a given value of density and internal energy,

$$T_{\min} \leq T(\bar{\phi}; \rho, e) \leq T_{\max} \quad (26)$$

The maximal linear eigenspace as well as its thermodynamic boundary, determined by Eq. (26), is illustrated in Figure 5.

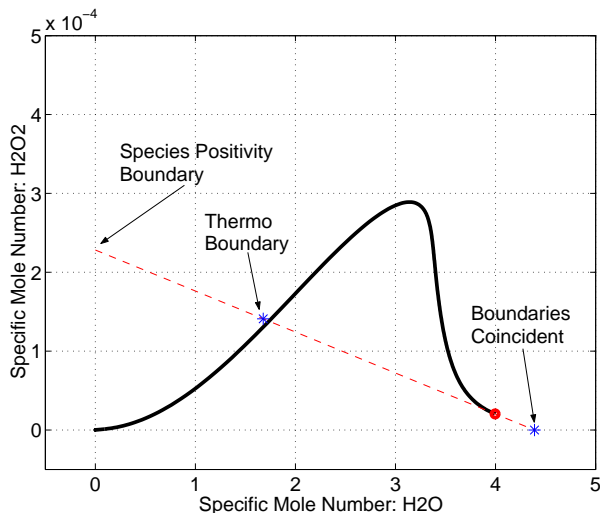


Figure 5: The dashed line represents the maximal extent of the slowest linear eigenspace subjected to positivity constraints. Asterisks represent the boundary with the additional constraint imposed by Eq. (26).

Each of the two thermodynamic boundary points will be used as initial data to Eq. (22). By using the time of arrival concept introduced earlier, each resulting trajectory is partitioned into two sets, before reaching \mathfrak{M}^1 and after.

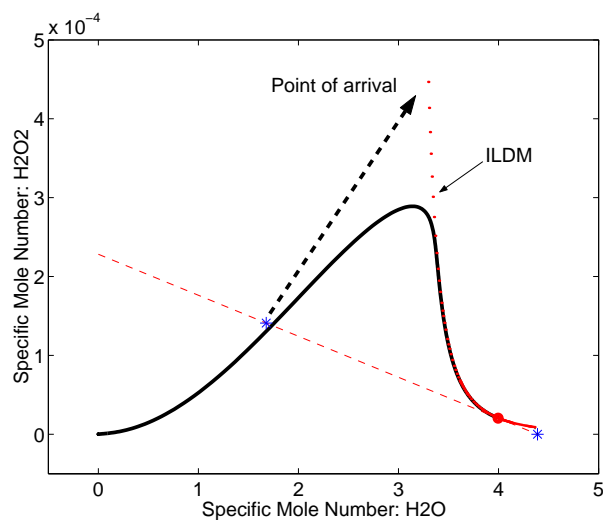


Figure 6: The dotted line represents the numerical solution to the one-dimensional ILDM. The deleted portion of the trajectory, corresponding to $\bar{\phi}(t < t^1)$, is replaced by an arrow from initial data (asterisk) to the point of arrival. (No arrow is shown between the asterisk to the right of the equilibrium, and the ILDM, because of their close proximity)

By truncating the initial portion of the trajectory, we are left with the piece that lies entirely in \mathfrak{M}^1 . Our numerical solution of \mathfrak{M}^1 is the union of the truncated trajectories from the two boundary points. This is illustrated in Figure 6.

Figure 6 demonstrates clearly that the original trajectory, also shown in Figure 4 and Figure 5, is attracted onto \mathfrak{M}^1 well before reaching the equilibrium position.

EXAMPLE: CONSTRUCTION OF HIGHER DIMENSIONAL ILDM

Computations of higher dimensional ILDMs proceed in exactly the same manner as in the previous section. We first solve the linear programming problem of finding the maximal linear eigenspace. The boundary of which is shrunken according to Eq. (26). Points on this boundary (denoted as the thermodynamic boundary) are evolved and the initial portion of each trajectory is truncated leaving behind the portion that lies entirely in \mathfrak{M}^k . This is shown in Figure 7. This algorithm can be parallelized in the obvious manner by means of domain decomposition of the thermodynamic boundary. Using this method, ILDMs of up to three dimensions (in chemical coordinates, not including the two trivial dimensions from the parameters of density and internal energy) have been computed successfully.

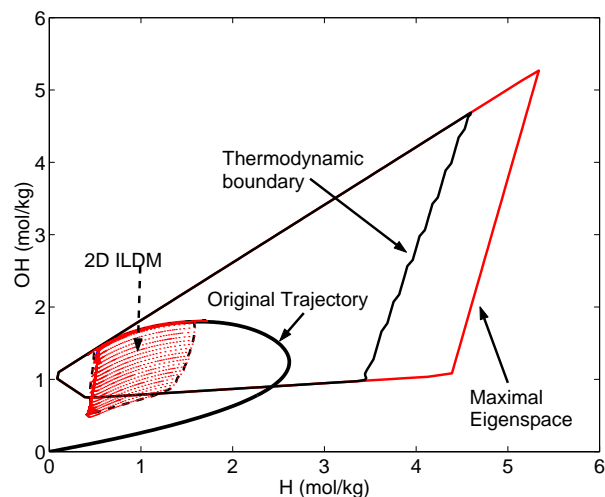


Figure 7: The components involved in the construction of a two-dimensional ILDM are shown.

ZND DETONATIONS AND THE ILDM

The common interpretation of ILDM as a reduction technique⁵ is that it identifies the chemical reactions whose timescales are commensurate with those from the fluid dynamics and decouples them from the rest. Theoretical foundations are not firm as far as we know, but valuable insights have been gained by studying the ILDM in the context of singular perturbation methods^{10,11}. We now know that the aforementioned decoupling is only approximate, and the identification of the slow manifold imprecise. Nevertheless, while the ILDM algorithm is not applicable to dynamical systems in general, it has had much success when applied to chemically reactive systems.

Because the fastest processes are explicitly ignored, it is important to get a handle on the error that results from this omission. A convergence study whereby we systematically increase the dimensionality of the ILDM is all but impractical.

In this section, we will apply the techniques of dimensional estimation to a one-dimensional steady (ZND) detonation with detailed chemistry¹².

The unsupported (CJ) ZND reaction zone structure for stoichiometric $\text{H}_2\text{-O}_2$ with 70% Ar dilution, initially at 6.67 kPa and 298 K is computed using an adaptation of the program ZND by Shepherd¹³.

The evolution of temperature and pressure for the ZND detonation is plotted as a function of the distance from the leading shock in Figure 8. The spatial profiles of the chemical species O_2 and H are shown in Figure 9. The position of the leading shock is located at 0 on the abscissa. It can be observed from these figures that the induction zone length for this detonation is approximately 0.15 cm.

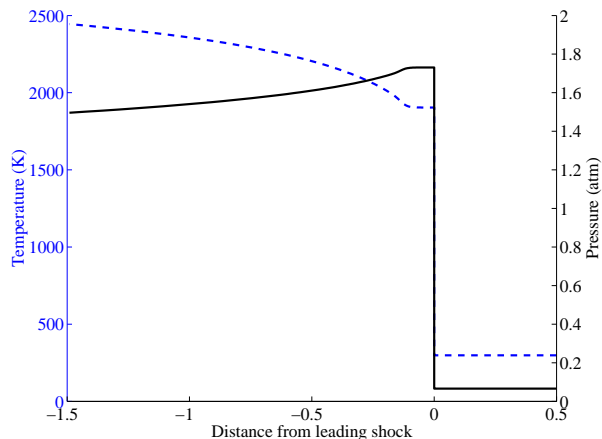


Figure 8 The steady ZND profiles for temperature and pressure are shown. Temperature is represented by the dashed line and pressure by the solid line. The induction zone length for the case under study is approximately 0.15 cm.

The detailed reaction mechanism¹⁴ used in this study consists of 12 species from 4 elements (H, O, N, Ar). Three of these species contain nitrogen, which is absent from our system. This leaves us with 9 active species and 3 elemental constraints for a maximum theoretical ILDM dimension of 6. A numerical representation of the ILDM is, as discussed before, a set of points which samples the ILDM. It is clearly impractical, loosely speaking, to mesh or tabulate a four- (or higher-) dimensional ILDM of any significant size.

Figure 10 gives us, for the first time, a quantitative answer to the question that is often raised but mostly unanswered: How many dimensions do we need? With this flow configuration, we can see, on the one hand, that a three-dimensional ILDM is sufficient to capture most of the flow-field except in a very thin layer behind the leading shock. On the other hand, one can argue that by using a one-dimensional ILDM, we have only ignored approximately the first five microseconds of the transients, justifying what initially seems to be an absurd amount of reduction as one-dimensional ILDMs are commonly used in the community.

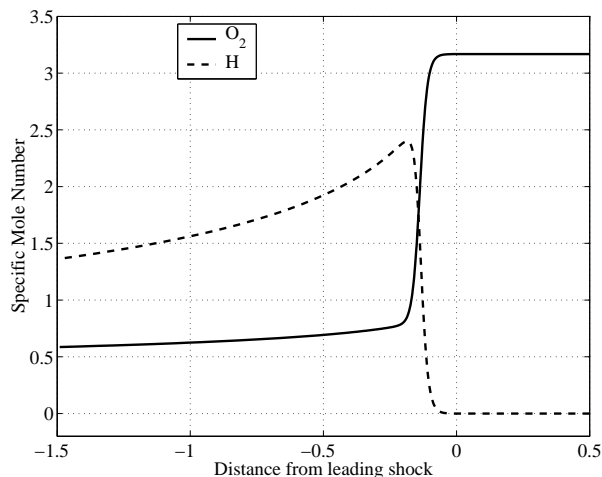


Figure 9: The steady ZND profiles for the specific mole numbers of O_2 and H are shown.

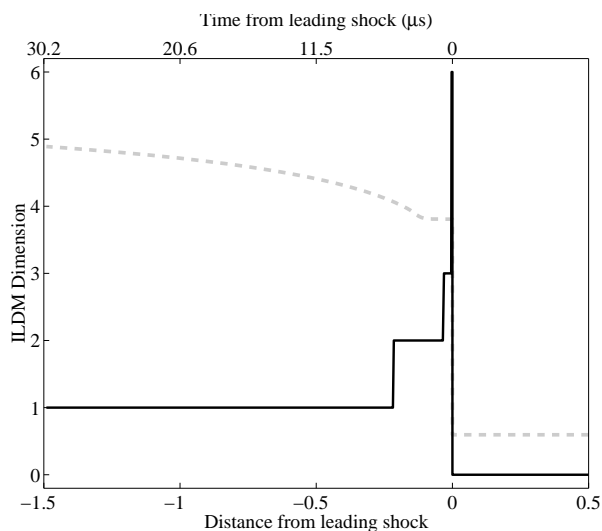


Figure 10: The ILDM dimension along the ZND trajectory is plotted. The temperature profile is superimposed on the plot as the dashed line.

The thin layer immediately behind the leading shock containing the extremely fast transients can be examined more closely in Figure 11. The rapid build-up of OH radical in the high-dimensional induction region is clearly displayed.

CONCLUDING REMARKS

Because of space limitations, many important details have been left out. Some of these are discussed below.

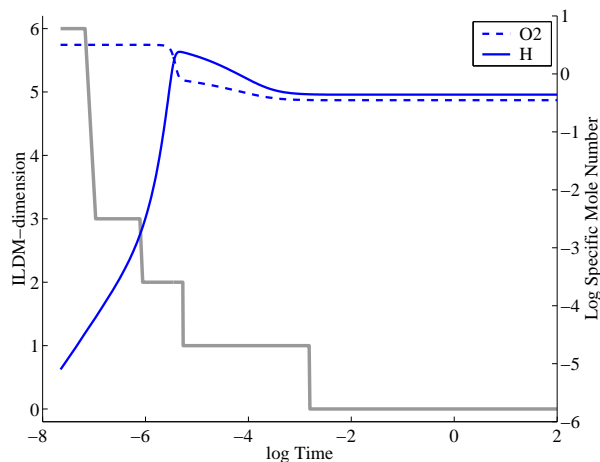


Figure 11: The species evolution and ILDM-dimension for the ZND detonation is shown in log scales.

The first is the issue concerning the noninvariance of ILDMs. Given a point $\bar{\phi}$ in \mathcal{M}^k , it does not follow that the evolution of $\bar{\phi}$ will remain on \mathcal{M}^k . This seems to be a contradiction to Eq. (21), but it isn't. First, we need to answer the question: What does arriving or reaching an ILDM mean? For an invariant (inertial¹⁵) manifold, trajectories are attracted and get exponentially close and the answer is clear. It is “on the manifold” when it is within some tolerance under some metric. For us, the arrival time has been carefully defined in Eq. (17) to be not the first time a trajectory reaches \mathcal{M} , but the last time. In other words, it “arrived” at the manifold as long as it doesn't wander afar ever after. Nevertheless, invariance is important because without it, a trajectory may never “reach” our manifold as it traverses the manifold ad infinitum. Furthermore using an ILDM in a numerical simulation implicitly constrains a reaction trajectory on it; any noninvariance leads to error. Fortunately, empirical evidence points in our favor. Chemical systems, which exhibit large separation of timescales, have ILDMs that well approximates the inertial slow manifold¹¹, forming the basis for making the invariance assumption.

How many dimensions should we choose? While choosing a high-dimensional manifold is theoretically more accurate, it isn't true in prac-

tice. Just like one wouldn't perform a strictly one-dimensional flow problem using a three dimensional solver, the problem is one of discretization: we can get a lot more information from one million one-dimensional cells, than looking at a one-dimensional slice of a 100^3 box.

As stated in the introduction, our goal is to adapt as much information as we can afford, and as little as we need. Pragmatic concerns limit our ability to manifolds of no more than two chemical dimensions (plus the two additional dimensions from the two parameters). Theoretically, as seen in Figure 10, we need more from the high-dimensionality of the induction zone. A solution, presented in Eckett², is to use a technique known as an "induction manifold" to bridge the gap between a low-dimensional ILDM and the missing transient.

¹ Maas, U. and Pope, S.B. "Implementation of Simplified Chemical Kinetics Based on Intrinsic Low-Dimensional Manifolds," *Combust. Flame*, Vol. 88, 1992, pp. 239-264

² Eckett, C.A. "Numerical and Analytical Studies of the Dynamics of Gaseous Detonations," CIT Thesis, Caltech, 2001.

³ Rastigejev Y., Singh S., Bowman C., Paoulcci S. and Powers J.M. "Novel modeling of hydrogen/oxygen detonation," AIAA-2000-0318, 38th AIAA Aerospace Sciences Meeting and Exhibit, Reno, Nevada, January 2000.

⁴ Singh, S. and Powers J.M., "Modelling Gas Phase RDX Combustion with Intrinsic Low Dimensional Manifolds," 17th International Colloquium on the Dynamics of Explosions and Reactive Systems, Heidelberg, Germany, July 1999.

⁵ Maas, U. "Efficient Calculation of Intrinsic Low-Dimensional Manifolds for the Simplification of Chemical Kinetics," *Computing and Visualization in Science*, Vol. 1, 1998, pp. 69-81

⁶ Courant and Hilbert. "Methods of Mathematical Physics, Volume I," John Wiley & Sons, 1989.

⁷ Golub, Gene H. and Van Loan, Charles F. "Matrix Computations. 3rd Edition" The Johns Hopkins University Press, 1996.

⁸ Schutz, B. "Geometrical methods of mathematical physics," Cambridge University Press, 1980

⁹ Rastigejev Y., Singh S., Bowman C., Paoulcci S. and Powers J.M. "Novel modeling of hydrogen/oxygen deto-

nation," AIAA-2000-0318, 38th AIAA Aerospace Sciences Meeting and Exhibit, Reno, Nevada, January 2000.

¹⁰ Rhodes C., Morari R. and Wiggins S. "Identification of low order manifolds: Validating the algorithm of Maas and Pope," *CHAOS*, Vol. 9, No. 1, 1999, pp. 108-123

¹¹ Kaper H.G. and Kaper T.J. "Asymptotic analysis of two reduction methods for systems of chemical reactions (Preprint)," ANL/MCS-P912-1001, Argonne National Laboratory, 2001

¹² Fickett W. and Davis W.C. "Detonation," University of California Press, 1979.

¹³ Shepherd, J.E. "AIAA Progress in Astronautics and Aeronautics," AIAA, New York, Vol. 106, 1986, pp. 263

¹⁴ Miller, J.A. and Bowman, C.T. "Mechanism and modeling of nitrogen chemistry in combustion," *Prog. Energy Combust. Sci.*, Vol. 15, 1989, pp. 287-338

¹⁵ Temam, R. "Infinite-Dimensional Systems in Mechanics and Physics," Springer-Verlag New York, Inc. 1997